HNPS Advances in Nuclear Physics

Vol 21 (2013)

HNPS2013

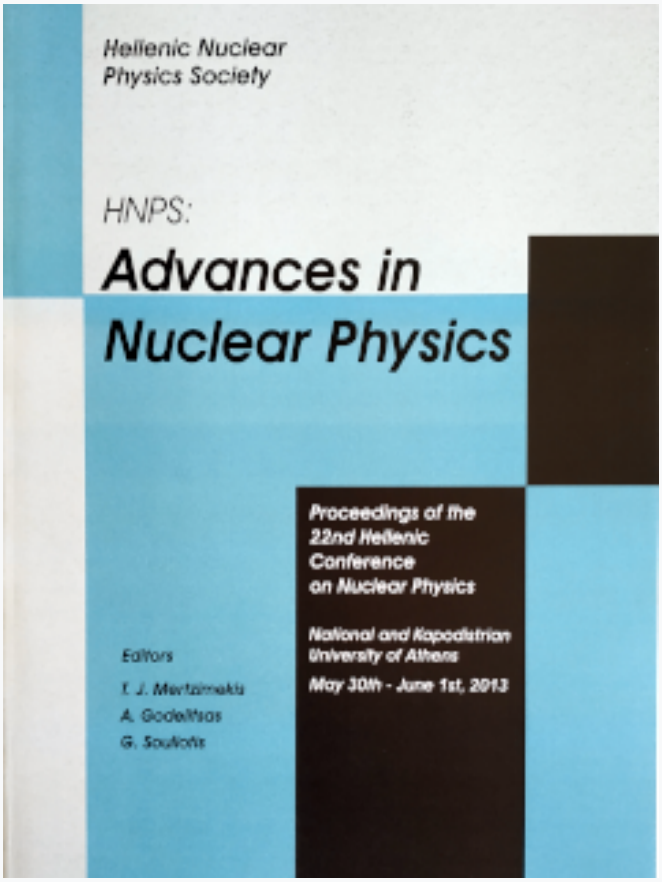

Studying background processes of the exotic neutrino-nucleus reactions

D. K. Papoulias, T. S. Kosmas

doi: 10.12681/hnps.1998

Studying background processes of the exotic neutrino-nucleus reactions

D.K. Papoulias[a], T.S. Kosmas[a]

[a] *Division of Theoretical Physics, University of Ioannina, GR 45100 Ioannina, Greece*

Abstract

The background processes of the flavour changing neutral current (FCNC) processes, predicted by various new-physics models to occur in the presence of nuclei, are examined by computing the relevant nuclear matrix elements within the context of the quasi-particle RPA using realistic strong two-body forces. Our main goal is to explore the role of the non-standard interactions (NSI) in the leptonic sector and specifically: (i) in lepton flavour violating (LFV) processes involving neutrinos ν_ℓ and $\tilde{\nu}_\ell$, $\ell = e, \mu, \tau$ and (ii) in charged lepton flavour violating (cLFV) processes involving the charged leptons ℓ^- or ℓ^+. As concrete nuclear system we have chosen the stopping target of $\mu^- \to e^-$ conversion experiment, i.e. the ^{48}Ti nucleus of the PRIME/PRISM experiment at J-PARC. This experiment has been designed to reduce the single event sensitivity down to 10^{-16}–10^{-18} in searching for charged lepton mixing events. We also present, stringent constraints on the flavour violating parameters entering the NSI Lagrangians that have been obtained by taking advantage of our detailed nuclear structure calculations and exploiting the present limits or the sensitivity of the proposed exotic $\mu^- \to e^-$ experiments.

Keywords: Non-Standard neutrino-nucleus reactions, Flavour-changing neutral-current, Nuclear structure calculations, Supernova neutrinos

1. Introduction

Coherent neutrino-nucleus scattering, which is the dominant reaction channel, is widely recognised as an excellent probe for exploring astrophysical phenomena [1–3], for deeper understanding the Supernova (SN) explosion mechanisms, as well as for investigating the interior of distant stars. Moreover, the exotic neutrino-nucleus reactions, offer interesting probes to search for new physics [4, 5] beyond the Standard Model (SM). Such possible, lepton flavour violating (LFV) processes have the form $\nu_\alpha(\tilde{\nu_\alpha}) + (A, Z) \to \nu_\beta(\tilde{\nu_\beta}) + (A, Z)$, where $\alpha \neq \beta$ [6–9]. The LFV parameters entering the latter flavour changing neutral current (FCNC) reactions, can be constrained from recent and future very sensitive experiments searching for exotic $\mu^- \to e^-$ conversion, like the COMET at J-PARC, JAPAN and the Project X at Fermilab, USA, using ^{48}Ti and ^{27}Al respectively, as nuclear targets [10, 11].

In the present work, as a first step we investigate in detail the response of the ^{48}Ti nucleus, due to its great experimental interest, according to the SM neutrino reactions [12, 13] represented by $\nu_\alpha(\tilde{\nu_\alpha}) + (A, Z) \to \nu_\alpha(\tilde{\nu_\alpha}) + (A, Z)$. We adopt the Donelly-Walecka method [14–16] and solve the BCS equations [17], to perform realistic and accurate cross sections calculations [18–20] within Supernova scenarios [21–24]. We also employ the method of fractional occupation probabilities (FOP) of the states [25, 26], based on analytic expressions, for evaluating the proton charge density distribution and the nuclear form factors [27–30], entering the coherent rate. To this contribution, we extend the previous studies, by introducing more parameters, increasing this way the number of "active" nucleons in the particular nuclear system. The consistency and reliability of the present work is checked by comparing our theoretical predictions with the available experimental data [31]. In Fig.1 we show some nuclear-level Feynman diagrams representing the exchange of a Z-boson between a lepton and a nucleon for the cases of ν-nucleus scattering in the SM (Fig.1(a)) and in the non-standard interactions of neutrinos with nuclei (Fig.1(b)). We also show the exchange of a Z-boson or a γ-photon in the $\mu^- \to e^-$ conversion, Fig.1(c) [4, 18]. The leptonic vertex in the cases of Fig.1(b),(c) is a complicated one.

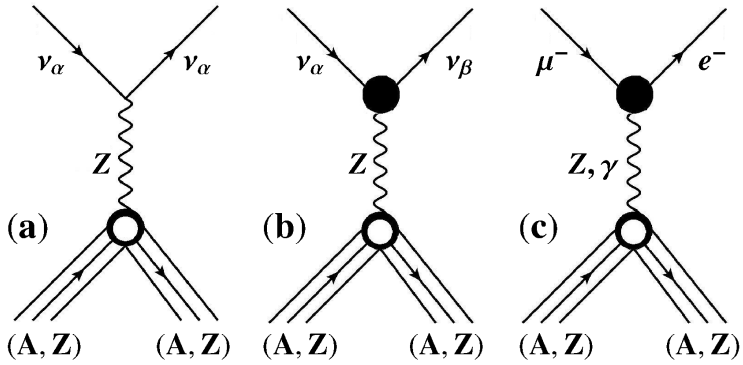

Figure 1: Nuclear level Feynman diagrams for: *(a)* SM Z-exchange neutral current ν-nucleus reactions, *(b)* non-standard Z-exchange ν-nucleus reactions, and *(c)* Z-exchange and photon-exchange $\mu^- \to e^-$ in the presence of a nucleus (muon-to-electron conversion). The non-standard (cLFV or LFV) physics enters in the complicated vertex denoted by the bullet $\bullet$. [5]

2. Brief description of the formalism

2.1. SM neutral current neutrino-nucleus cross sections

At low and intermediate neutrino energies, considered in the present study, the SM ν-nucleus reactions may be described by the effective (quark-level) interaction Lagrangian [7]

$$\mathcal{L}_{\rm SM} = -2\sqrt{2}G_F \sum_{\substack{f=u,d \\ \alpha=e,\mu,\tau}} g_P^f \left[\bar{\nu}_\alpha \gamma_\rho L \nu_\alpha\right] \left[\bar{f}\gamma^\rho P f\right], \tag{1}$$

where $g_L^u = \frac{1}{2} - \frac{2}{3}\sin^2\theta_W$ and $g_R^u = -\frac{2}{3}\sin^2\theta_W$ are the left- and right-handed couplings of the u-quark to the Z-boson and $g_L^d = -\frac{1}{2} + \frac{1}{3}\sin^2\theta_W$ and $g_R^d = \frac{1}{3}\sin^2\theta_W$ are the corresponding couplings of the d-quark (θ_W is the Weinberg mixing angle) [15]. The polar-vector couplings of protons and neutrons to the Z boson (see Fig.1), are written in terms of the Weinberg mixing angle θ_W as: $g_V^p = 2(g_L^u + g_R^u) + (g_L^d + g_R^d) = \frac{1}{2} - 2\sin^2\theta_W$ and $g_V^n = (g_L^u + g_R^u) + 2(g_L^d + g_R^d) = -\frac{1}{2}$, respectively.

In the Donnelly-Walecka multipole decomposition method, the neutral-current, double differential SM cross section from an initial $|J_i\rangle$ to a final $|J_f\rangle$ nuclear state reads [1, 15]

$$\frac{d^2\sigma_{i\to f}}{d\Omega\, d\omega} = \frac{G_F^2}{\pi}\frac{\epsilon_i \epsilon_f}{(2J_i+1)}\left(\sum_{J=0}^{\infty}\sigma_{\rm CL}^J + \sum_{J=1}^{\infty}\sigma_{\rm T}^J\right), \tag{2}$$

where ϵ_i (ϵ_f) is the initial (final) neutrino energy. The cross sections $\sigma_{\rm CL}^J$ (for the Coulomb-longitudinal operators) and $\sigma_{\rm T}^J$ (for the tensor operators) are defined in [15] and are written in terms of the matrix elements (ME) of seven basic irreducible tensor operators, which in our convention are [14, 16]

$$\langle j_1 || T_i^J || j_2 \rangle = e^{-y} y^{\beta/2} \sum_{\mu=0}^{n_{max}} \mathcal{P}_\mu^{i,\,J} y^\mu, \qquad i = 1, \cdots, 7. \tag{3}$$

Therefore, their evaluation is necessary for performing nuclear cross sections calculations. These coefficients, $\mathcal{P}_\mu^{i,\,J}$, have been computed recently in Refs.[14, 16]. In this paper we focus in the special case of the dominant coherent channel where only $g.s \to g.s$ transitions occur, thus $\epsilon_i = \epsilon_f \equiv E_\nu$ and only the Coulomb operator, $T_0^0 \equiv \hat{\mathcal{M}}_{00}$ (see, Eq.(8)), should be taken into account. Then, the differential cross section with respect to the scattering neutrino angle becomes [12, 13]

$$\frac{d\sigma}{d\cos\theta} = \frac{G_F^2}{8\pi} E_\nu^2 \left(1 + \cos\theta\right) Q_W^2 F^2(q^2), \tag{4}$$

where the weak charge is defined as $Q_W = \left[\left(1 - 4\sin^2\theta_W\right) Z - N\right]$. The kinematics of the reaction, imply that the magnitude of the three momentum transfer, written in terms of the incoming neutrino energy E_ν and the scattering angle θ (laboratory frame), is [26]

$$q^2 = 4E_\nu^2 \sin^2\frac{\theta}{2}. \tag{5}$$

However, from an experimental physics point of view, experiments are more sensitive to the kinetic energy of the recoiling nucleus given by $T = q^2/2M$, rather than the orientation of the scattering neutrino. Thus, expressing the differential cross section with respect to the nuclear recoil energy T, in the low energy approximation $T \ll E_\nu$, one finds [23, 30]

$$\frac{d\sigma}{dT} = \frac{G_F^2 M}{4\pi}\left(1 - \frac{M T}{2E_\nu^2}\right) Q_W^2 F^2(q^2), \tag{6}$$

where M stands for the mass of the target nucleus. It can be seen from Eqs.(4,6) that the nuclear form factor has been taken into account, which from a nuclear physics point of view cannot be neglected, due to the finite nuclear size. In the rest of this work, we describe an effective method towards obtaining the form factor which is compared with the simple shell-model predictions through nuclear cross sections calculations.

More precise cross sections calculations become possible by explicitly solving the BCS equations [17] and the differential cross section can be cast in the form [26]

$$\frac{d\sigma}{d\cos\theta} = \frac{G_F^2}{2\pi} E_\nu^2 \left(1 + \cos\theta\right) \left|\langle g.s.||\hat{\mathcal{M}}_{00}(q)||g.s.\rangle\right|^2, \tag{7}$$

where $|g.s.\rangle$ is the nuclear ground state (for spin-zero nuclei $|g.s.\rangle = |J^\pi\rangle \equiv |0^+\rangle$). For this particular case the $g.s. \to g.s.$ transition ME is given by

$$\langle g.s.||\hat{\mathcal{M}}_{00}(q)||g.s.\rangle = \frac{1}{2}\left[\left(1 - 4\sin^2\theta_W\right) Z F_Z - N F_N\right]. \tag{8}$$

2.2. Non-standard neutral current neutrino-nucleus cross sections

The ν-nucleus NSI (see Fig.1b), are described by an effective quark-level NSI Lagrangian of the form (energies $\ll M_Z$) [2, 3, 5, 7, 9]

$$\mathcal{L}_{NSI} = -2\sqrt{2} G_F \sum_{\substack{f=u,d \\ \alpha,\beta=e,\mu,\tau}} \epsilon_{\alpha\beta}^{fP} \left[\bar{\nu}_\alpha \gamma_\rho L \nu_\beta\right] \left[\bar{f}\gamma^\rho P f\right], \tag{9}$$

where three light neutrinos $\nu_{\alpha,\beta}$ with Majorana masses are assumed, f is a first generation quark and $P = \{L, R\}$ are the chiral projectors. Note that the latter Lagrangian contains two types of couplings relative to the strength of the Fermi constant G_F. These include the non-universal (NU) terms proportional to $\epsilon_{\alpha\alpha}^{fP}$ as well as flavour-changing (FC) contributions originating from the $\epsilon_{\alpha\beta}^{fP}$, $\alpha \neq \beta$ and holds that $\epsilon_{\alpha\beta}^{fP} = \epsilon_{\alpha\beta}^{fL} + \epsilon_{\alpha\beta}^{fR}$ for the polar-vector couplings and $\epsilon_{\alpha\beta}^{fP} = \epsilon_{\alpha\beta}^{fL} - \epsilon_{\alpha\beta}^{fR}$ for the axial-vector couplings. The nuclear physics aspects of the FCNC reactions are studied by transforming the Lagrangian of Eq.(9) to the nuclear level where the hadronic current contains the neutral-current nucleon form factors which are functions of the four-momentum transfer [19].

The corresponding NSI coherent differential cross section with respect to the outgoing neutrino scattering angle θ that arises from the NSI Lagrangian of Eq.(9) is [5]

$$\frac{d\sigma_{(NSI)}}{d\cos\theta} = \frac{G_F^2}{2\pi} E_\nu^2 \left(1 + \cos\theta\right) \left|\langle g.s.||G_V^{NSI}(q)||g.s.\rangle\right|^2, \tag{10}$$

The $g.s. \to g.s.$ NSI transition nuclear matrix element now takes the form [5]

$$\begin{aligned}\left|\langle g.s.||G_V^{NSI}(q)||g.s.\rangle\right|^2 = &\left[\left(2\epsilon_{\alpha\alpha}^{uV} + \epsilon_{\alpha\alpha}^{dV}\right) Z F_Z(q^2) + \left(\epsilon_{\alpha\alpha}^{uV} + 2\epsilon_{\alpha\alpha}^{dV}\right) N F_N(q^2)\right]^2 \\ &+ \sum_{\alpha\neq\beta}\left[\left(2\epsilon_{\alpha\beta}^{uV} + \epsilon_{\alpha\beta}^{dV}\right) Z F_Z(q^2) + \left(\epsilon_{\alpha\beta}^{uV} + 2\epsilon_{\alpha\beta}^{dV}\right) N F_N(q^2)\right]^2,\end{aligned} \tag{11}$$

$(\alpha, \beta = e, \mu, \tau)$. In an exact analogous way with the SM cross sections, the corresponding differential cross sections with respect to the nuclear recoil energy T_N are written as [5, 7, 8]

$$\frac{d\sigma_{(NSI)}}{dT_N} = \frac{G_F^2 M}{\pi}\left(1 - \frac{M T_N}{2E_\nu^2}\right)\left|\langle g.s.||G_V^{NSI}(q)||g.s.\rangle\right|^2 . \tag{12}$$

The upper limits on the NSI parameters $\epsilon_{\alpha\beta}^{fP}$ that have constrained by the corresponding experiments can be found in [6]. Table 1 lists the upper limits on the NSI parameters $\epsilon_{\mu e}^{fP}$ that have been derived by exploiting the extremely high sensitivity of the proposed $\mu^- \to e^-$ conversion experiments in Ref.[5].

	COMET	Mu2e	Project-X	PRIME
$\epsilon_{\mu e}^{fP} \times 10^{-6}$	3.70	2.87	0.52	0.37

Table 1: Upper limits on the NSI parameters $\epsilon_{\mu e}^{fP}$ and the corresponding ratios $R_{\nu_\mu \leftrightarrow \nu_e}$ for the FC $\nu_\mu \leftrightarrow \nu_e$ reaction channel resulting from the sensitivity of the $\mu^- \to e^-$ conversion experiments.

2.3. Evaluation of the form factors

The electromagnetic form factors $F_{Z(N)}$ for protons (neutrons) enter the aforementioned SM and NSI scattering cross sections of the previous subsections due to the CVC theory. These form factors are functions of the three momentum transfer i.e. $F_{Z(N)} \equiv F_{Z(N)}(q^2)$ may be predicted within various models.

From a nuclear structure perspective the form factors can be obtained by solving iteratively the BCS equations to determine the BCS probability amplitudes, $V_j^{p(n)}$ of the $j-$th single nucleon level that enters the nuclear nuclear factor [17]

$$F_{N_n}(q^2) = \frac{1}{N_n}\sum_j [j]\,\langle g.s.||j_0(qr)||g.s.\rangle\left(V_j^{p(n)}\right)^2 \tag{13}$$

where $[j] = \sqrt{2j+1}$, $N_n = Z$ (or N) and $j \equiv (n, \ell)j$ are the quantum numbers of the h.o. orbits included in the assumed model space. The chosen active model space consists of the lowest 15 single-particle j-orbits, $j \equiv (n, \ell, 1/2)j$ without core [5]. The required monopole (pairing) residual interaction, obtained from a Bonn C-D two-body potential (strong two-nucleon forces), was slightly renormalized with the two parameters $g_{\rm pair}^{p,n}$ for proton (neutron) pairs and the other required nuclear parameters are listed in Table 2.

Nucleus	model-space	b	Δ_p^{th} (MeV)	Δ_n^{th} (MeV)	$g_{\rm pair}^p$	$g_{\rm pair}^n$
^{48}Ti	15-levels (no core)	1.952	1.9111	1.5573	1.0564	0.9989

Table 2: The adopted nuclear structure parameters for the construction of the nuclear $g.s.$ for the ^{48}Ti isotope.

We note that, in the approximation of $F_Z \approx F_N$ and $|J_i^\pi\rangle = |g.s.\rangle \equiv |0^+\rangle$ for the ground state, Eq.(7) coincides with Eq.(4).

The proton density distribution is well measured by electron scattering experiments [31], and models exist to calculate the overall form factor. The most complete treatment is [27] and the form factor used is

$$F(q^2) = \frac{3j_1(qR_o)}{qR_o}\exp\left[-\frac{1}{2}(qs)^2\right], \tag{14}$$

where R_0 stands for the nuclear radius written in terms of the nuclear skin thickness, $s = 0.5$, as $R_0^2 = R^2 - s^2$ with $R = 1.2\,A^{1/3}$ fm. In the next section we use the latter form factor to compare the consistency and accuracy of our nuclear structure BCS method.

For other interesting approximations including the Nuclear Shell-Model and the fractional occupation probalilities (FOP) methods the reader is referred to [26].

3. Results and discussion

One of the most interesting connections of our present calculations with ongoing and future neutrino experiments is related to supernova neutrino detection. As it is known, in supernova explosions most of the energy is released by neutrino emission. Then, the total neutrino flux arriving at a terrestrial detector, $\Phi(E_\nu)$, as a function of the SN neutrino energy E_ν, reads [23, 24]

$$\Phi(E_\nu) = \sum_\alpha \Phi_{\nu_\alpha}(E_\nu) = \sum_\alpha \frac{N_{\nu_\alpha}}{4\pi\, d^2}\, \eta_{\nu_\alpha}^{\rm SN}(E_\nu), \tag{15}$$

($\alpha = e, \mu, \tau$) where N_{ν_α} is the number of (anti)neutrinos emitted from a supernova source at a typical distance (here we used $d = 8.5\,$kpc) and $\eta_{\nu_\alpha}^{\rm SN}$ denotes the energy distribution of the (anti)neutrino flavour α. We assume that the emitted SN-neutrino energy spectra $\eta_{\nu_\alpha}^{\rm SN}(E_\nu)$ resemble Maxwell-Boltzmann distributions

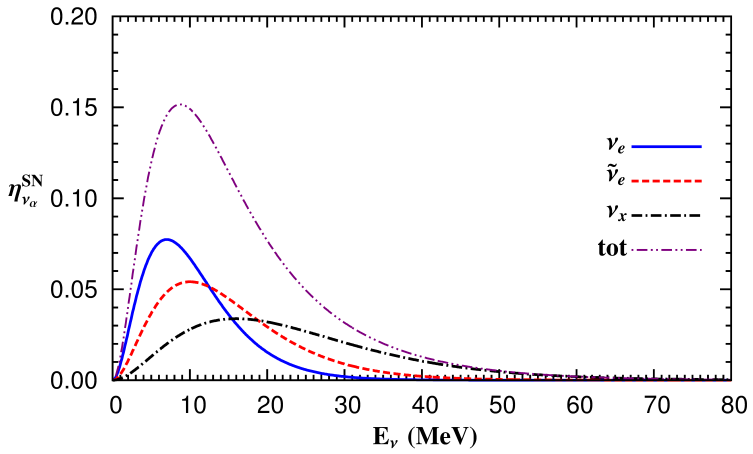

Figure 2: Maxwell-Boltzmann spectra for the three neutrino flavours used in the present calculations.

that depend on the temperature T_{ν_α} of the (anti)neutrino flavour ν_α ($\tilde{\nu}_\alpha$) as

$$\eta_{\nu_\alpha}^{\rm SN}(E_\nu) = \frac{E_\nu^2}{2T_{\nu_\alpha}^3} e^{-E_\nu/T_{\nu_\alpha}}\,, \tag{16}$$

($T_{\nu_e} = 3.5$MeV, $T_{\tilde{\nu}_e} = 5.0$MeV, $T_{\nu_x,\tilde{\nu}_x} = 8.0$MeV, $x = \mu, \tau$). The number of emitted neutrinos N_{ν_α} can be readily found from the mean neutrino energy $\langle E_{\nu_\alpha}\rangle = 3T_{\nu_\alpha}$ and the total energy released from a supernova explosion, $U = 3 \times 10^{53}$erg [21, 22].

From experimental physics perspectives, it is also interesting to make predictions for the differential event rate of a ν-detector [20, 23, 24]. The usual expression for computing the yield in events is based on the neutrino flux, Φ_{ν_α}. To include the NSI of neutrinos with nuclei, the yield in events $Y_{\lambda,\nu_\alpha}(T_N)$, is defined as [5, 23, 24]

$$Y_{\lambda,\nu_\alpha}(T_N) = N_t \int \Phi_{\nu_\alpha}\, dE_\nu \int \frac{d\sigma_{\lambda,\nu_\alpha}}{d\cos\theta}\, \delta\left(T_N - \frac{q^2}{2M}\right) d\cos\theta\,, \tag{17}$$

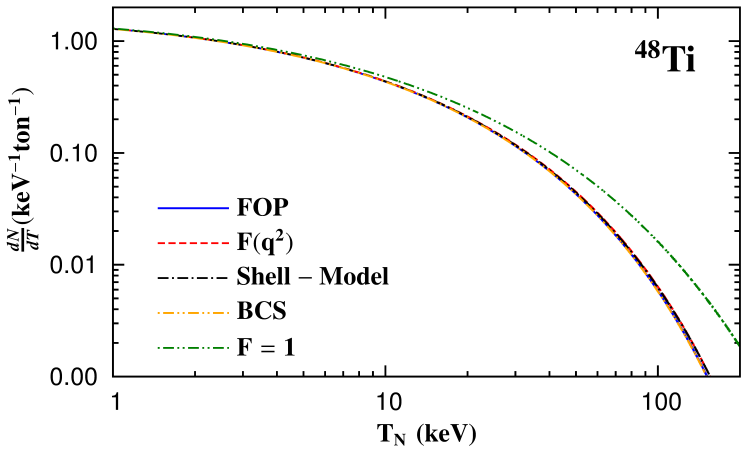

Figure 3: The expected differential event rate for a terrestrial nuclear detector that consists of 1 tone ^{48}Ti.

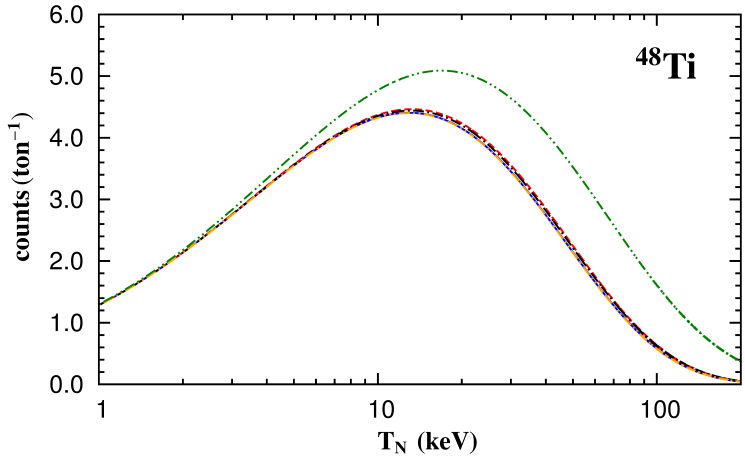

Figure 4: The response function for a terrestrial nuclear detector that consists of 1 tone ^{48}Ti.

where N_t is the total number of nuclei (atoms) in the detector material. Assuming a detector filled with one tone ^{48}Ti, we evaluated differential event rates $Y_{\lambda,\nu_\alpha}(T_N)$ and the response function (see Fig.3 and Fig.4 respectively) for several supernova scenarios.

We find that all nuclear methods used in the present work (i.e. Shell-Model, FOP, BCS and that of Eq.(14)), yield similar results. However, for the approximation of unity form factor in which the nuclear physics details of the reaction are considered negligible, we found an excess on the results for both differential event rate of Eq.(17) and response function (i.e. Eq.(17) times the nuclear recoil energy T_N).

One of the most important quantities from an experimental point of view is to measure the total number of events for the particular reaction. To this purpose, we apply the present formalism to make predictions for the total number of ν-nucleus events to be detected over a threshold by a terrestrial experiment. By integrating Eq.(17) over a nuclear threshold $T_{N_{\rm thres.}}$ we obtain the results presented in Fig.5.

We find that for a nuclear threshold set at $T_{N_{\rm thres.}} = 1$keV and taking into account our realistic nuclear structure calculations we end up with about 14 events per tone of a ^{48}Ti terrestrial detector. As expected, the number of events decreases smoothly for higher thresholds. Again, we stress that neglecting the nuclear physics aspects of the reaction an important excess for the expected events of the order of 30% is found.

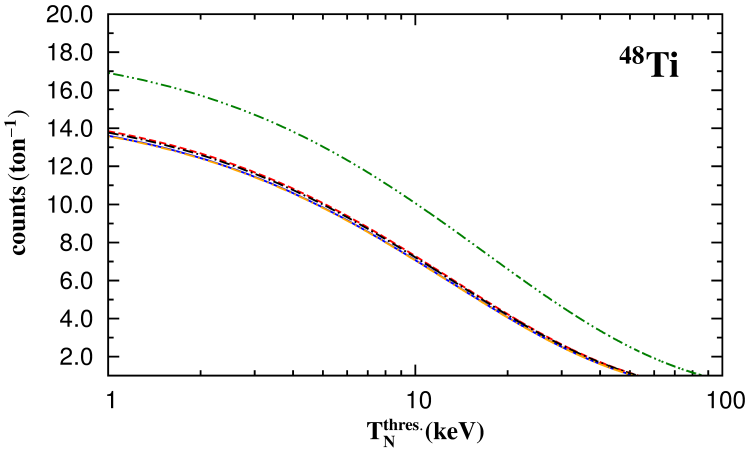

Figure 5: Number of total counts over threshold for a nuclear detector filled with 1 tone ^{48}Ti.

4. Summary and Conclusions

In this work, we reported a general method for making realistic coherent neutrino-nucleus cross sections calculations. It is worth mentioning that, especially when we deal with Supernova neutrinos (or neutrinos with higher energies originating from other sources) taking into account the momentum variation of the form factor is of significant importance. Comparing with other nuclear methods (like the simple shell-model and fractional occupation probabilities) and other mean field approximations (or other where the form factor is set equal to unity), we ended up with more reliable results. We conclude that since for the dominant coherent channel of the ν-nucleus reactions the contribution to the cross section is mainly due to ν-neutron scattering, the BCS method yields the most precise results. The present calculations strongly indicate that for the case of Supernova neutrino-nucleus reactions offer measurable rates. We stress however, that a deviation from the SM prediction could indicate new physics beyond the SM. We finally mention that our study can be also applied to make predictions for other type of experiments including stopped-pion muon neutrino sources for which due to the high neutrino intensity, event rates may be in the tens per year even for kilogram-scale detectors. Such results will be published soon elsewhere.

References

[1] T.W. Donnelly and R.D. Peccei, Phys. Rept. **50** (1979) 1.
[2] P.S. Amanik, G. M. Fuller and B. Grinstein, Astropart. Phys. **24** (2005) 160.
[3] P.S. Amanik and G.M. Fuller, Phys. Rev. **D 75** (2007) 083008.
[4] F. Deppisch, T.S. Kosmas and J.W.F. Valle, Nucl. Phys. **B 752** (2006) 80.
[5] D.K. Papoulias and T.S. Kosmas, Phys. Lett. **B 728** (2014) 482-488
[6] S. Davidson, C. Pena-Garay, N. Rius, and A. Santamaria, JHEP **03** (2003) 011.
[7] J. Barranco et. al., JHEP **0512** (2005) 021.
[8] K. Scholberg, Phys. Rev. **D 73** (2006) 033005.
[9] J. Barranco, O.G. Miranda, C.A. Moura and J.W.F. Valle, Phys. Rev. **D 73** (2006) 113001.
[10] Y.G. Cui et al. (COMET Collaboration), KEK Report 2009-10.
[11] R. Bernstein and G. Kribs, talk at 2012 Project X Physics Study (PXPS12), Fermilab, June 14-28, 2012 Chicago USA.
[12] D.Z. Freedman, et. al., Annu. Rev. Nucl. Sci. **27** (1977) 167.
[13] A. Drukier and L. Stodolsky, Phys. Rev. **D 30** (1984) 2295.
[14] D.K. Papoulias and T.S. Kosmas, J. Phys. Conf. Ser. **410** (2013) 012123.
[15] T.W. Donnelly and J.D.Walecka, Nucl. Phys. **A 274** (1976) 368.
[16] V.Ch. Chasioti and T.S. Kosmas, Nucl. Phys. **A 829** (2009) 234.
[17] T.S. Kosmas et. al., Nucl. Phys. **A 570** (1994) 637.
[18] T.S. Kosmas and J.D. Vergados, Phys. Rept. **264** (1996) 251.
[19] T.S. Kosmas, S. Kovalenko and I. Schmidt, Phys. Lett. **B 511** (2001) 203; Phys. Lett. **B 519** (2001) 78.
[20] K.G. Balasi, E Ydrefors and T.S. Kosmas, Nucl. Phys. **A 868** (2011) 82.

[21] K. Hirata, et al., Phys. Rev. Lett. **58** (1987) 1490; R.M. Bionta, et al., Phys. Rev. Lett. **58** (1987) 1494.
[22] Y. Giomataris, J.D. Vergados, Phys. Lett. **B 634** (2006) 23.
[23] C.J. Horowitz, K.J. Coakley, and D.N. McKinsey, Phys. Rev. **D 68** (2003) 023005.
[24] M. Biassoni and C. Martinez, Astropart. Phys. **36** (2012) 151.
[25] T.S. Kosmas and J.D. Vergados, Nucl. Phys. **A 536** (1992) 72.
[26] D.K. Papoulias and T.S. Kosmas, Proc. 21st Symposium of the Hellenic Nuclear Physics Society 2013, May 30-31, Athens, Greece, in press.
[27] J. Engel, Phys. Lett. **B 264** (1991) 114.
[28] T.S. Kosmas and J.D. Vergados, Phys. Lett. **B 215** (1988) 460.
[29] T.S. Kosmas and J.D. Vergados, Nucl. Phys. **A 510** (1990) 641.
[30] J. Monroe and P. Fisher, Phys. Rev. **D 76** (2007) 033007.
[31] H. De Vries et. al., At. Data and Nucl. Data Tables **36** (1987) 495536.